zinc sulphide, while only 1 to 2 cracks are nucleated around indentations on the coated surface (Fig. 2). The size of the plastic impression is however the same in both cases. Examination of the coating surface showed that the cracks do not, or only partially, extend into the coating surface, indicating that the crack is nucleated *in the substrate*. It should be pointed out that the protection offered by the coating depends on its thickness. No statistically significant reduction in the radial crack length, nor in the number of cracks nucleated, was observed for specimens coated with a 2 μm thick thorium oxide coating.

Two explanations can be put forward to explain the observed reduction of the radial crack length due to the thorium oxide coating.

(1) Since the thermal expansion coefficient of thorium oxide is lower than that for zinc sulphide, compressive stresses are generated in the composite structure on cooling down from the deposition temperature. This beneficial effect will disappear at high indenter loads, where the magnitude of the pre-existing stresses is small compared with the induced stresses.

(2) The presence of a "stiffer" coating with a high interfacial strength will reduce the displacements in the coating–substrate interface, providing the coating does not fail at lower stress levels than the substrate. This will reduce the tensile stresses responsible for crack propagation.

A theoretical model is being developed to calculate the effect of various coating parameters on the stress field generated by localized loading conditions.

Acknowledgements

Helpful discussions with Drs J. E. Field and J. T. Hagan are gratefully acknowledged. Specimens were kindly provided by S. W. Warren, ITT Components Group, Harlow. This study was sponsored by the Ministry of Defence (Procurement Executive).

References

1. S. VAN DER ZWAAG, J. T. HAGAN and J. E. FIELD, *J. Mater. Sci.* **15** (1981) 2965.
2. S. PALMQUIST, *Jernkoterets Ann.* **141** (1957) 300.

Received 2 February
and accepted 27 February 1981

S. VAN DER ZWAAG
Physics and Chemistry of Solids,
Cavendish Laboratory,
Madingley Road,
Cambridge, UK

Normal and anomalous fatigue crack propagation (FCP) of thermoplastic polymers

As a result of the increasing use of thermoplastic polymers as structural components in the past ten years, increasing interest has been shown in their fatigue crack propagation (FCP) behaviour. Most of the work conducted in this area was concentrated on amorphous polymers such as polystyrene (PS) or polymethylmethacrylate (PMMA). The most important result is the validity of a relation of the type

$$\frac{da}{dN} = A\Delta G^n = A\left(\frac{\Delta K^2}{E}\right)^n, \qquad (1)$$

where da/dN is the crack growth rate, A and n are empirical constants, ΔG is the energy release rate, ΔK is the stress intensity and E is Young's modulus.

On the other hand, only limited knowledge is available on the behaviour of semicrystalline materials. Hertzberg *et al.* [2, 3] have shown that significant differences exist between amorphous and crystalline polymers. Crystallinity clearly provides a higher resistance against the growth of fatigue cracks.

The purpose of this investigation is to obtain a more detailed insight into the fatigue properties of semicrystalline polymers. Therefore FCP-tests with a constant triangular load amplitude ΔF were conducted with low molecular weight polyethylene (LMWPE) (molecular weight, $\bar{M}_w$ = 100 000), high molecular weight polyethylene (HMWPE) ($\bar{M}_w$ = 450 000), polyamid-6 (PA6),

0022–2461/81/102915–05$02.50/0

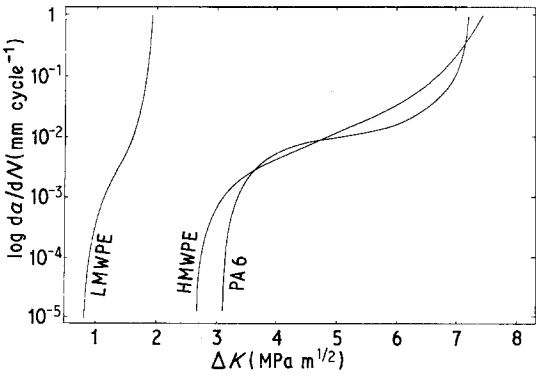

Figure 1 Variation of da/dN with ΔK for LMWPE, HMWPE and PA6 (molecules with zig-zag conformation).

polypropylene (PP), polyetrafluoroethylene (PTFE), and polybutene (PB-1). All tests have been conducted at ambient temperatures with compact tension specimens of 5 mm thickness, prepared with a razor notch. The frequency of loading was 0.1 Hz in order to eliminate the influence of a temperature rise in front of the crack tip. At higher frequencies this could lead to thermal softening in the plastic zone [4, 5].

During cyclic loading all the materials examined formed a zone of plastic deformation in front of the crack tip into which the crack has to propagate. The properties of the material in this zone dictate the growth of the fatigue cracks.

The da/dN–ΔK curves for the two types of PE and PA6 (Fig. 1) show the form known from the literature (Equation 1), [1–3, 6, 7]. With increasing stress intensity, ΔK, the crack propagation rate, da/dN, increases steadily until unstable crack growth occurs. Differences in the resistance to FCP are related to the different degrees of strain hardening of the polymers.

The curves measured for PP, PTFE and PB-1 apparently show a totally different slope from those shown by PE and PA6 (Fig. 2). Their FCP behaviour can be divided into four regions:

Region 1: $\Delta K < \Delta K_0$, no crack growth;

Region 2: $\Delta K_0 \leqslant \Delta K < \Delta K_1$, delayed stable crack growth;

Region 3: $\Delta K_1 \leqslant \Delta K < \Delta K_c$, accelerated stable crack growth;

Region 4: $\Delta K_c \leqslant \Delta K$, unstable crack growth.

These regions of different FCP behaviour are also evident in the morphology of the fracture surfaces, as examined by SEM (Fig. 3). In Region 1 there is no crack growth. Region 2 is associated with the fatigue striations which become smaller in the direction of crack propagation and which are not dependent on the number of cycles (Fig. 3a). Region 3 shows striations with a direct corre-

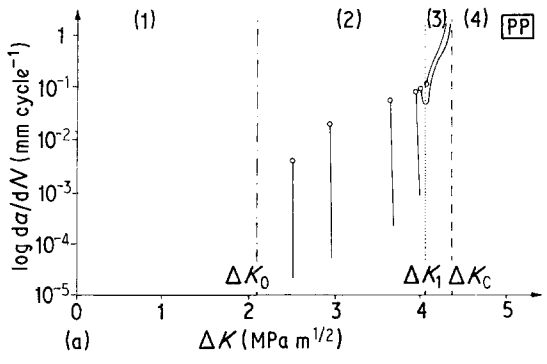

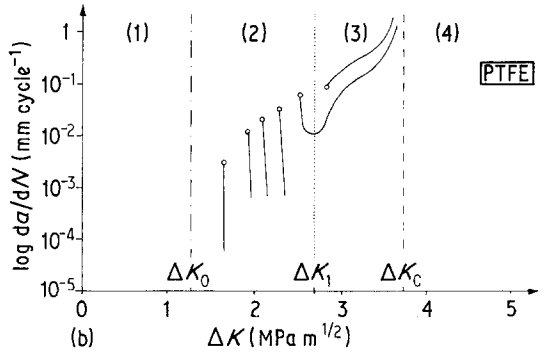

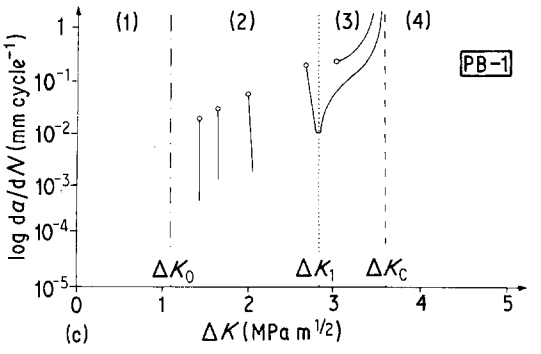

Figure 2 Variation of da/dN with ΔK for (a) PP, (b) PTFE, and (c) PB-1 (molecules with helical conformation). The curves were obtained using specimens exposed to different initial amplitudes of stress intensity (○).

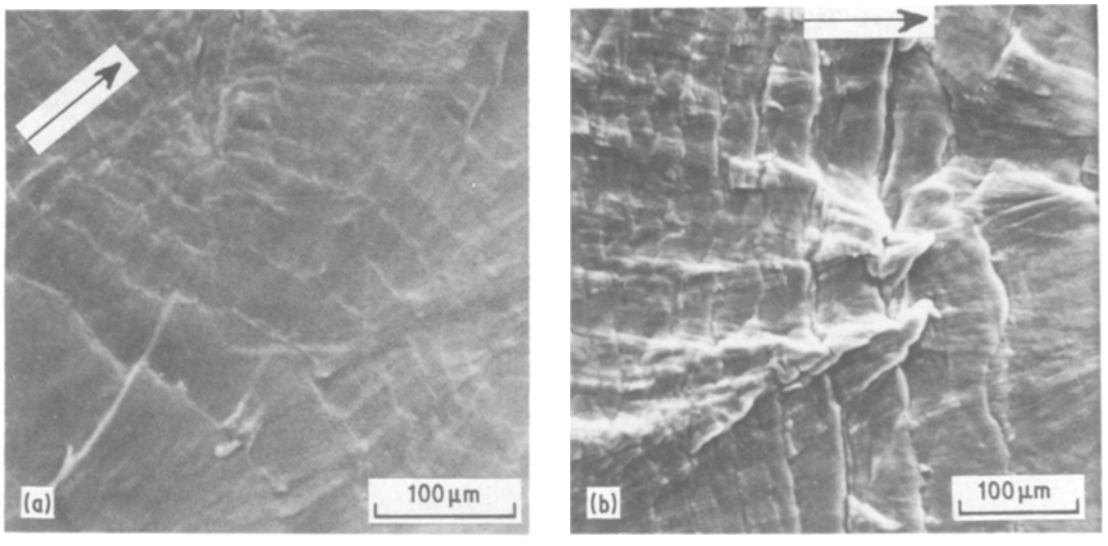

Figure 3 Fracture surfaces of PP, showing the different regions of FCP. (a) Stable delayed crack growth, (b) stable accelerated crack growth and (c) unstable crack growth (→ indicates the direction of crack growth).

lation to the number of cycles. These striations become wider with increasing crack propagation (Fig. 3b). Finally, Region 4 shows a surface typical of a region of brittle unstable fracture (Fig. 3c).

Of special interest is the anomalous delayed FCP of Region 3. The crack growth rate, da/dN, decreases to zero with increasing number of cycles. Plotting an envelope through the crack initiation rates of Regions 2 and 3 (Fig. 4), a curve is obtained which indicates that for the first cycle the behaviour of the polymers with anomalous FCP is similar to that of PE and PA6; it is only in the successive cycles that crack retardation becomes effective.

Tensile tests can possibly provide further information on the particular behaviour which must be taking place in the plastic zone ahead of the crack tip. One interpretation may come from a subdivision of the strain, ϵ, into a reversible portion, ϵ_{rev}, and an irreversible (plastic) portion. Fig. 5 shows a plot of ϵ_{rev} against ϵ for the materials examined and a significant difference in behaviour is evident between PE and PA6 on one side and the polymers showing the anomalous behaviour on the other. The former show only a negative curvature:

$$d^2\epsilon_{rev}/d\epsilon^2 < 0; \quad (2)$$

i.e., the reversible deformation increases only a little with increasing total deformation, ϵ. On the other hand, the curves for PP, PTFE, and PB-1 show positive curvature at higher strains:

$$d^2\epsilon_{rev}/d\epsilon^2 > 0; \quad (3)$$

i.e., the reversible portion of deformation increases significantly.

The established relation between the energy release rate, G_{IC}, the yield stress, σ_y, and the crack opening displacement, δ_c, is:

$$G_{IC} = \sigma_y \delta_c. \quad (4)$$

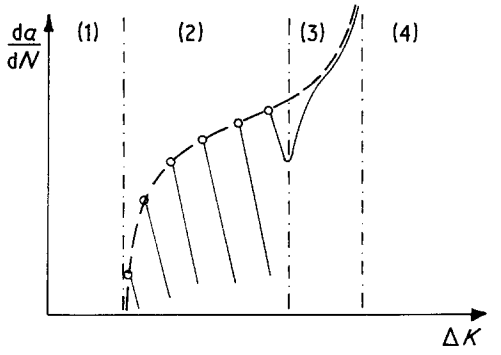

Figure 4 Variation of da/dN with ΔK for PP, PTFE and PB-1 for one cycle, $N = 1$ (dotted line), and for many cycles, $N \rightarrow \infty$.

Equation 4 is assumed to be valid for subcritical crack opening displacements in fatigue, such that

$$\Delta G = \sigma_y \delta, \tag{5}$$

and for which $\delta/2$ produces a crack propagation of length approximately Δa. If δ contains a considerable reversible portion, δ_{rev}, (proportional to ϵ_{rev} of the tensile test) crack growth is retarded. For the first cycle:

$$\frac{\Delta G_1}{\sigma_y} = (\delta - \delta_{rev})_1 = 2\,\Delta a_1. \tag{6}$$

Together with the crack propagation, Δa_1, ΔG increases for the second cycle to:

$$\Delta G_2 = \Delta\sigma_a^2\,\pi\,(a_0 + \Delta a_1), \tag{7}$$

where $\Delta\sigma_a$ is the amplitude of external stress and a_0 is the initial crack length.

At the same time the strain hardening at the crack tip causes an increase, $\Delta\sigma_y$, in the yield stress. The relation for the crack growth Δa_2 during the next cycle is then given as:

$$\frac{\Delta G_2}{\sigma_y + \Delta\sigma_y} = (\delta - \delta_{rev})_2 = 2\,\Delta a_2. \tag{8}$$

For normal crack growth $\Delta a_1 < \Delta a_2$ is valid, while for retarded crack propagation $\Delta a_1 > \Delta a_2$ is characteristic.

For $\Delta a_1 < \Delta a_2$ the increase of the energy release rate ΔG (Equation 7) caused by the crack growth Δa_i, is higher than the rise of the yield stress $\Delta\sigma_{yi}$ caused by strain hardening in the plastic zone. Thus the crack propagation rate da/dN increases steadily. Differences in the resistance to FCP, such as exist between amorphous and crystalline polymers, are due to different yield stress and strain hardening abilities. The reversible component of the crack opening displacement, δ_{rev}, is not of importance, as its increase is negligible.

The range in which $\Delta a_1 > \Delta a_2$ for PP, PTFE and PB-1, is caused by the significant increase of the reversible part of deformation ($d^2\epsilon_{rev}/d\epsilon^2 > 0$). The effective crack opening displacement ($\delta - \delta_{rev}$) for the crack propagation becomes smaller and the crack propagation rate da/dN decreases.

In all the thermoplastic polymers a very pronounced molecular alignment was present at the crack tip. However, anomalous FCP behaviour was found only in polymers with a helical structure. It is supposed that the high reversibility of strain, and consequently of this anomaly, is caused by this molecular conformation after the molecules have been aligned parallel to the tensile stress. This hypothesis is presently under investigation.

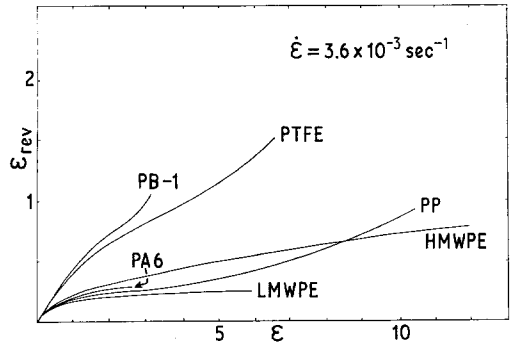

Figure 5 Reversible portion of deformation ϵ_{rev} plotted against total deformation, ϵ, as obtained for tensile tests of all the materials used for this investigation.

Acknowledgement

The authors wish to thank the Deutsch Forschungsgemeinschaft (Project Ho325/14) for supporting this work.

References

1. M. O. SPEIDEL, "High-temperature Materials in Gas Turbines", edited by P. R. Sahm and M. O. Speidel (Elsevier Publishing Co., Amsterdam, New York and Oxford, 1974) p. 207.
2. R. W. HERTZBERG, J. A. MANSON and W. C. WU, STP 530 ASTM (1973) p. 391.
3. J. A. MANSON and R. W. HERTZBERG, *CRC Crit. Rev. Macromol. Sci.* **1** (1973) 433.

4. G. MENGES and E. ALF, *J. Elast. Plast.* 7 (1975) 47.
5. R. J. CRAWFORD and P. P. BENHAM, *Polymer* **16** (1975) 908.
6. J. M. SCHULTZ, "Treatise on Material Science and Technology" Vol. 10, Part B (Academic Press, New York and London, 1977) p. 599.
7. F. X. de CHARENTENAY, F. LAGHOUATI and J. DEWAS, 4th International Conference on Defects, Yield and Fracture of Polymers, Cambridge, March 1979, Paper 6.

Received 3 February
and accepted 27 February 1981

A. SANDT
E. HORNBOGEN
Institut für Werkstoffe,
Ruhr-Universität Bochum,
Postfach 102148,
D-4630 Bochum,
West Germany

Oxidation behaviour of aluminium alloys containing magnesium and lithium

The thermal oxidation of certain Al alloys has been studied by new methods [1, 2] in the last few years. There is an increasing interest in understanding the structural and compositional changes occurring at metal–gas-phase boundaries. Heat-treatment is one of the most common technological procedures used in aluminium semi-fabrication. Depending on the composition of the bulk material, compositional and structural changes may occur at the metal–gas-phase boundary.

The question investigated by electron microscopy and thermogravimetry was: how is the oxi dation behaviour of Mg-containing alloys is influenced by Li?

The compositions of the alloys examined are given in Table I. The alloys were prepared from high purity base materials. The homogenized alloys were rolled to 0.5 mm and for electron microscopy purposes the samples were solution heat-treated and then cold-water quenched before electropolishing. *In situ* oxidation experiments were conducted in an AEI EM 7 high voltage electron microscope (HVEM) using 500 kV and a vacuum of 2×10^{-4} Pa at 500° C for 0.5 h. The heating rate used was about 100° C min^{-1}. Other samples prepared for electron microscopy were heat-treated at 10^5 Pa in air at 500° C for 4 h. Morphological and structural observations were evaluated and compared to the results obtained by thermogravimetric (TG) measurements. The TG measurements were made in the low-temperature furnace of a Mettler thermobalance (No 212). The surface area of the samples was 42 cm^2. The material was heat-treated in a dried air flow of 16 l h^{-1} at 350° C

TABLE I Composition of the alloys in wt%

Alloy	Zn	Mg	Li
Al–Zn–Mg	5.0	2.1	–
Al–Zn–Mg + Li	5.0	2.1	0.19

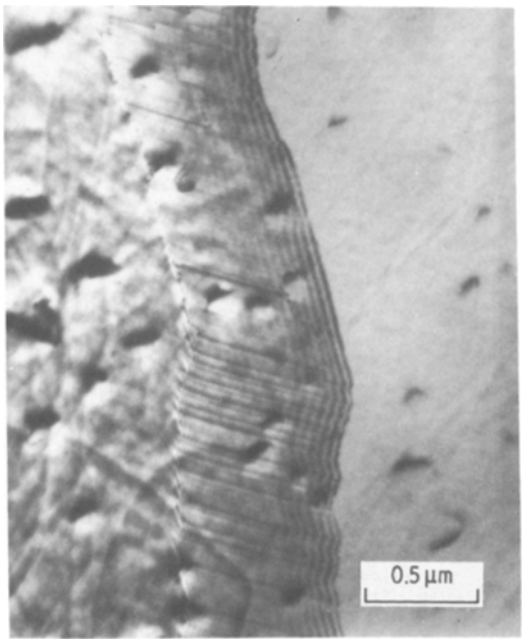

Figure 1 Oxide crystals on the surface of an Al–Zn–Mg alloy heat-treated at 500° C for 1 h in air at 2×10^{-4} Pa.

0022–2461/81/102919–04$02.40/0